Whitepaper

PREDICTING *FATIGUE PERFORMANCE* OF FIBER REINFORCED PLASTIC GEARS

To be successful in gear applications it is key to accurately predict short– and long–term mechanical performance, such as static strength due to misuse or stall torque and durability performance with root fracture as a failure mode.

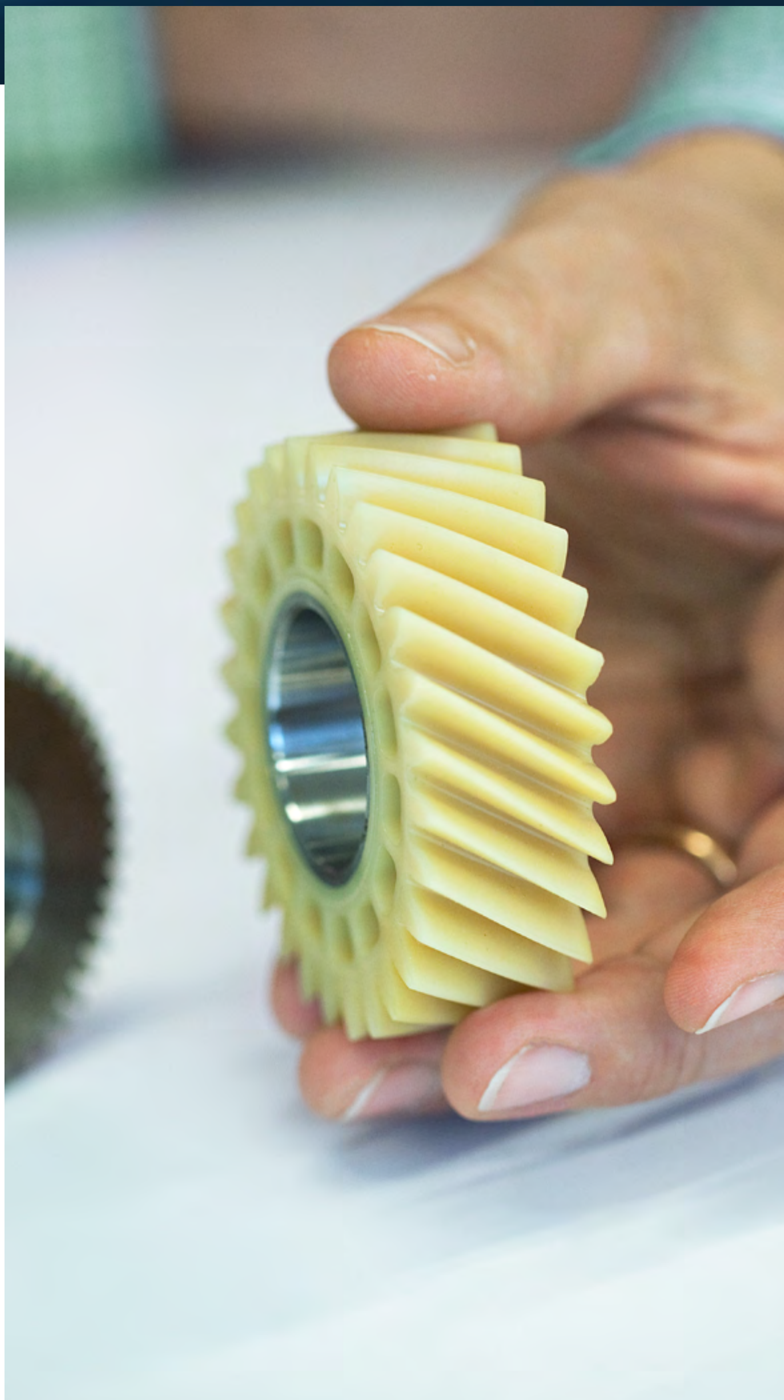

Applications with many different load cases, including temperature variations, result in a complex combination of failure modes. Because of this complexity, one tends to perform dedicated application tests in each design phase and converge to a final design in an iterative way.

However, with fundamental material knowledge and gear–application know–how one can combine test results obtained via simplified tests, such as standard tensile bar fatigue testing or simplified gear test results, into a model that provides accurate lifetime predictions. This can significantly reduce the time and costs that are involved in developing such applications.

This white paper is about ongoing work on the approach to predict root fatigue failure, including its temperature dependence based on non–isothermal durability measurements on a gear tester. It describes a framework to predict the fatigue performance of plastic gears, validated on an experimental case study. Long–term durability data of fiber reinforced plastic gears is obtained by using a dedicated gear tester and advanced finite element analysis, including the local fiber orientation in combination with the intrinsic material behavior. It is then used to predict the gear's failure mode and its corresponding torque level.

However, not in all cases does one have the opportunity to take fiber orientation into account. In these cases, an isotropic elastoplastic material model is often used. To do so, stress–strain data measured on injection molded ISO 527–1A tensile bars is used and converted into an elastic–plastic material model. In these injection molded bars, the fibers are highly oriented parallel to the loading direction. So, to take into account the often, more randomly distributed fiber orientation in a part, such as a gear, it is common to multiply the measured stiffness and strength of the tensile bar with a certain factor between 0.6 and 0.8, depending on the amount of fibers.

Figure 1a

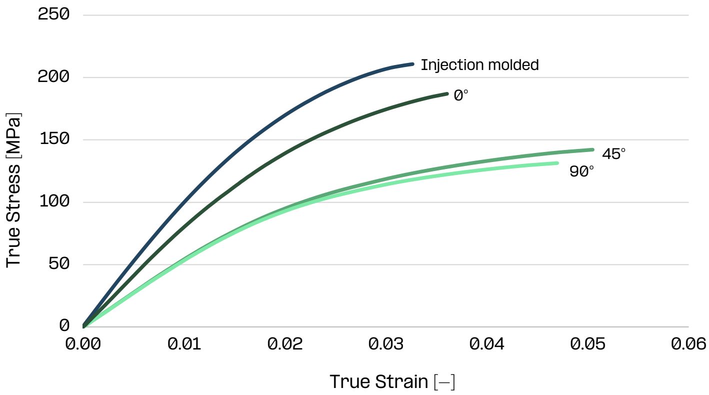

Figure 1b

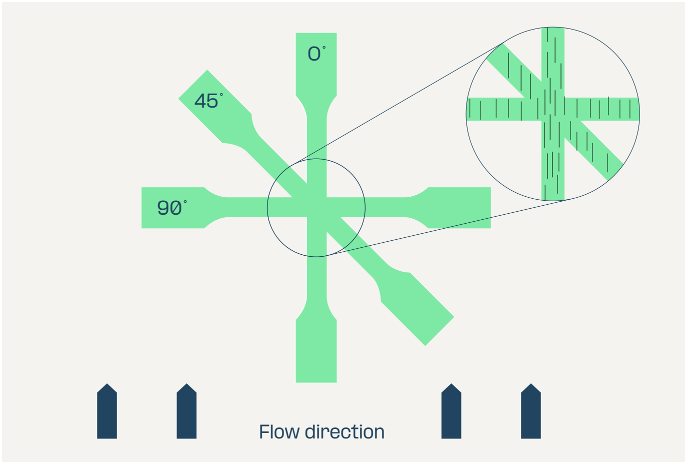

Figure 1 a/b
a) Stress–strain curves for a typical 30%wt fiber reinforced thermoplastic at room temperature and b) schematic illustration of oriented tensile bars milled from an injection molded plaque.

The selection of the magnitude of this factor is commonly based on experience. Its actual value, which can only be obtained after reverse engineering on actual part experiments, is highly dependent on part geometry, gating locations and loading– and boundary– conditions. To exclude those dependencies upfront and therefore increase the accuracy of the predictions, one should take into account the local fiber orientation.

The influence of anisotropy on the material behavior is calibrated from stress–strain data measured at specimens with various average fiber orientations. The specimens are milled from an injection molded plaque under various angles with respect to the flow direction, as illustrated in Figure 1, according to ISO 527–1B. Combined with information about the local fiber orientation in the center of the specimens, measured with a μ–CT scan, a mean–field homogenization method allows us to reverse engineer the fiber and polymer matrix properties, such as modulus, yield–stress and hardening modulus.

DURABILITY

Mechanical stress related to long–term fatigue performance of engineering plastics is commonly attributed to two failure mechanisms: plasticity–controlled failure or crack–growth controlled failure. For cyclic loading with relatively large amplitude and large number of cycles, as is the case for most glass fiber reinforced gears, lifetime will be dominated by crack–growth controlled failure. For this specific failure mode, small initial flaws, e.g. caused by processing, handling, or the presence of fillers, result in stress concentrations within a loaded material. These flaws initiate and subsequently propagate a craze or crack that finally causes failure. Fatigue lifetime in this region can be described using a power law:

EQUATION 1

$$\sigma(N_f) = c_f \cdot N_f^{-1/m}$$

In which σ is the applied stress, N_f the number of cycles to failure, *m* the slope of the Paris law and c_f a pre–factor that defines the stress that results in a lifetime of 1 s.

It is generally observed that the slope m is independent of temperature and the dependence of the lifetime can be incorporated via adjusting the pre–factor only.

EQUATION 2

$$\sigma(N_{f,}T) = c_f\,(T) \cdot N_f^{-1/m}$$

To model the temperature dependence of the mechanical performance of polymers, often an Arrhenius relationship is used, suggesting a linear dependence of the evolution of the logarithm of c_f with the reciprocal of temperature:

EQUATION 3

$$c_f\,(T) = c_{f,ref,geom} \cdot \mathrm{h}(T) = c_{f,ref,geom} \cdot \exp\,(\Delta U/R\,(1/T - 1/T_{ref}))$$

Where $c_{f,ref,geom}$ is the reference value for a certain geometry with specific test conditions at a certain reference temperature, ΔU is the activation energy and *R* the gas constant. In this work the applicability of this relation will be investigated in more detail.

MATERIALS, TEST METHODS AND ANALYSIS TECHNIQUES

Materials

Stanyl TW271F6 was used in all tests. All tests are performed with samples that contained no moisture at the start of the test. For the durability tests samples with solid lubricant added were used.

The gears were injection molded in a 2–cavity mold, designed for a 30%wt glass–fiber reinforced gear, which offers good compensation for the shrinkage during molding. Each gear is injection molded via six gates as displayed in Figure 2. The quality level of the gears after molding is 12 according to ISO 1328. The module of the gears was 1 mm, with a face width of 6 mm. The pitch diameter was 30 mm, which brings the number of teeth to 30. The addendum was 1 mm, the dedendum 1.25 mm with a root radius of 0.25 mm. In the durability tests, the driven and driver gear have both the same geometry. The nominal value of the center distance is 30 mm, but is adjusted prior to each test to ensure an initial backlash of 0.3 mm, based on measured maximum tip diameters of each gear.

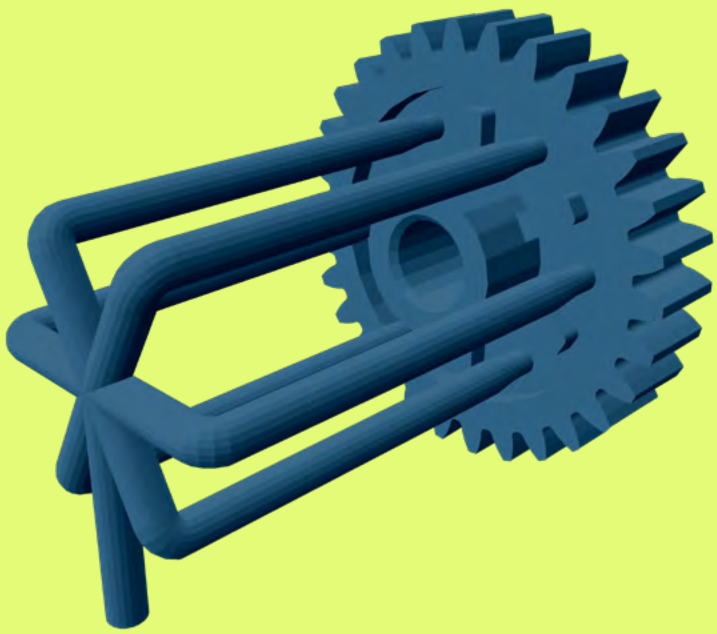

Figure 2
Illustration of the gear geometry including runner and 6–point gate system.

Experimental setups

To perform durability tests, a custom–built machine was used, displayed in Figure 3. It consists of two motors where one is rotating the gear at a given speed while the other one brakes to ensure a constant output torque at the driven gear. The setup was placed inside a chamber to control the environmental temperature. The tests are performed within a range of environmental temperatures. Due to friction the local tooth temperature increases until a steady–state situation has developed. The local tooth temperate is measured via an infrared sensor.

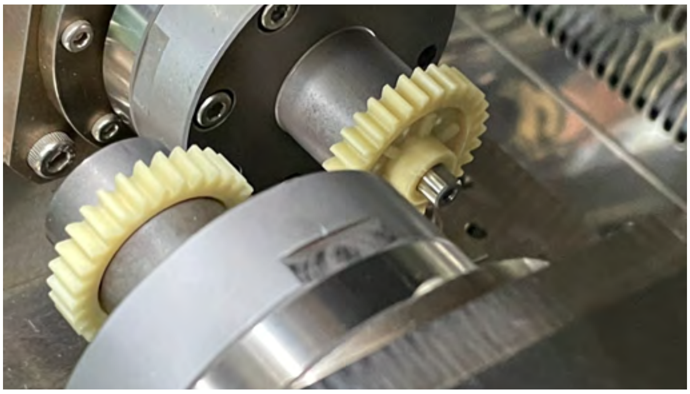

Figure 3
Image of the custom build gear durability tester.

Predicting local fiber orientation

Due to the injection molding process there exists a non–uniform local fiber orientation distribution in the gear. Figure 4 shows the first major orientation direction of the local fibers due to the injection molding simulation. It is clear that there are some differences in the amount of alignment, indicated by the grey color variations. A darker color indicates a majority of alignment in that particular direction, a lighter color indicates that a smaller fraction is aligned. These differences in fiber orientation will also cause differences in local stiffness and strength.

In most cases it shows highly aligned fibers parallel to the root of the teeth. But a more pronounced difference is observed at the weld line locations. Because during the injection molding, two flow fronts of molten polymer will meet each other at a location between two injection points, forming a weld–line. This is in this case at the root between two teeth at six locations in the gear. As a result, the fiber orientation at those locations is not oriented parallel to root of the teeth and there will be a difference in stiffness and strength at these weld line locations compared to a location without weld line.

Figure 4
Illustration of the predicted local fiber orientation in the gear.

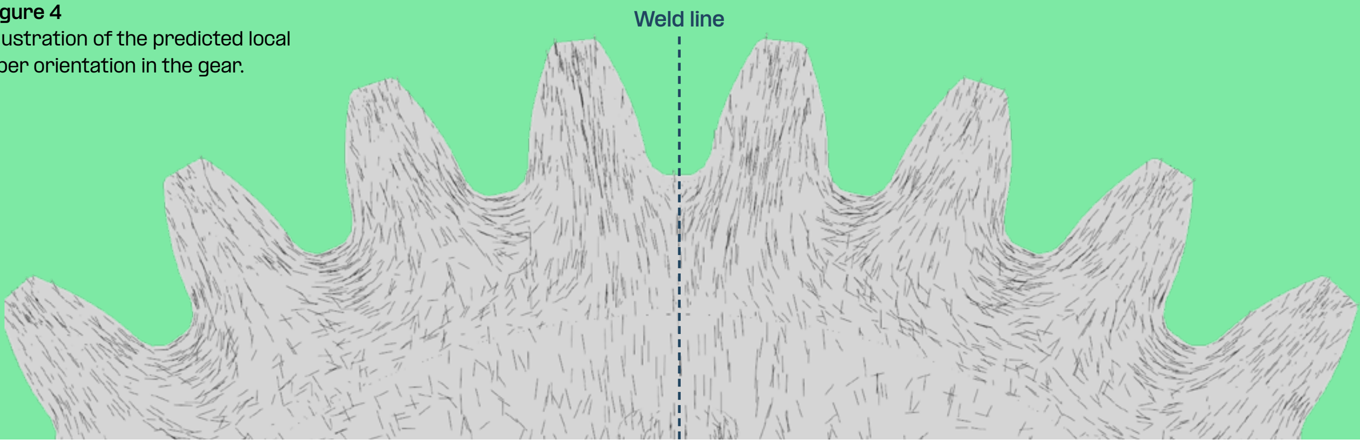

Simulations

In order to predict root fatigue, root stresses were calculated with KISSsoft, according to VDI 2736: 2013 (Method C). The contact analysis module was used with an application factor (K_a) of 1.0. Stress–strain data was measured for a large temperature range on an ISO 527–1A tensile specimen with a high fiber orientation parallel to the loading direction. It was chosen to not take into account the local fiber orientation.

Instead, an average uniform fiber orientation in the tooth of the gear is assumed, for this the stresses of the stress–strain curve are multiplied with a factor. A typical value for a 30%wt fiber reinforced polymer is 0.75, however this is strongly dependent on local gear geometry and gate locations. From the reduced stress–strain curves, the Young's modulus was calculated as a function of temperature.

GEAR DURABILITY

Gear durability tests were performed for different torque levels and various environmental temperatures and the lifetime was recorded. The results are provided in Figure 5, and it shows the lifetime is severely affected by the applied torque level and to a lesser extent by environmental conditions. For example, on one hand, for most cases, decreasing the load from 3Nm to 2Nm increases the lifetime with approximately a factor 10. However, increasing the temperature by 100°C only reduces lifetime by a factor 4.

Figure 5a

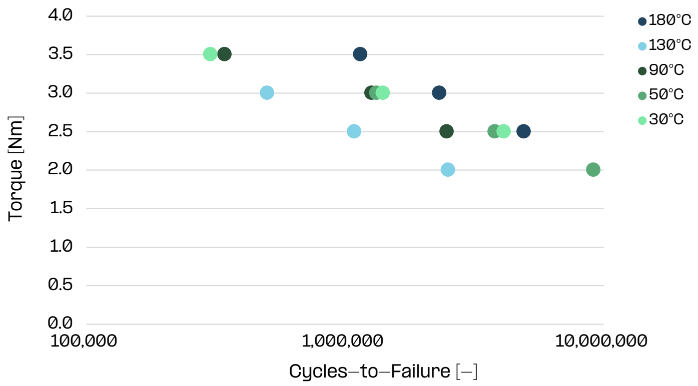

Figure 5b

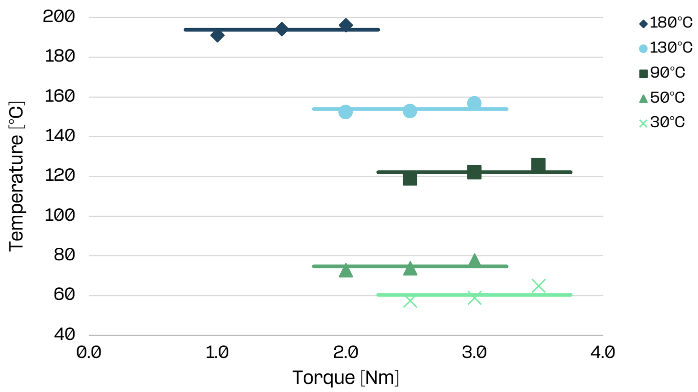

Figure 5 a/b
a) Gear durability results for various torque levels measured at various environmental temperatures and b) resulting average local tooth temperatures.

As can be seen in Figure 5b, the latter is related to the fact that the average tooth temperature is much higher than the environmental temperature set in the temperature chamber due to additional heat generation by friction at the tooth contacts. Even despite the presence of the solid lubricant, the local tooth temperature is on average approximately 20–30°C higher than the environmental temperature. As expected the temperature also increases with applied torque level, but since it is only a minor increase, the average tooth temperatures (dashed lines) are used for the remainder of the work for the sake of simplicity.
To properly account for the gear geometry, the applied torque levels should be transformed to root stresses. In order to incorporate the effect of temperature, the modulus of the material was adjusted in KISSsoft. Hence, as shown in Figure 6a, it was chosen to plot the root stresses for certain applied torque versus the modulus. The advantage of this approach is that the resulting root stresses are now applicable for any material of which the modulus is known. It shows that for a specific modulus, the root stresses increase with increasing torque level.

Furthermore, for the highest torque levels the dependence on modulus displays three regions:

- At low moduli, the root stress is more or less independent of modulus.
- At intermediate moduli, the root stress increases strongly with increasing modulus.
- For high moduli the root stress is again independent of modulus.

This can easily be explained by the fact that as long as the contact ratio under load at maximum stress remains constant, the modulus will only affect the maximum deflection of the tooth and the root stress remains dictated by the applied torque level only.

For low moduli (region I), the maximum contact ratio is already achieved and root stress is not affected by modulus. However, when the modulus is further increased, the teeth can become sufficiently rigid that it starts to affect the contact ratio and simply a larger fraction of the applied torque will be carried by lesser teeth, increasing the root stresses (region II). For sufficiently high moduli (region III), the contact ratio is again no longer affected and the root stress is again constant. And since the deflection of the teeth depends on torque level, the magnitude of the moduli where you might see these transitions will depend on the applied torque level.

Based on the results in Figure 6a, the root stresses can be extracted to match the gear experiments, here performed by linear interpolation. This allows to transform the torque versus cycles (T–N) plot (Figure 5a) to root stress versus cycles (S–N) as shown in Figure 6b. One might appreciate that the data represented in the S–N plot shows a much stronger dependence on temperature than the data in the T–N plot.

Figure 6a

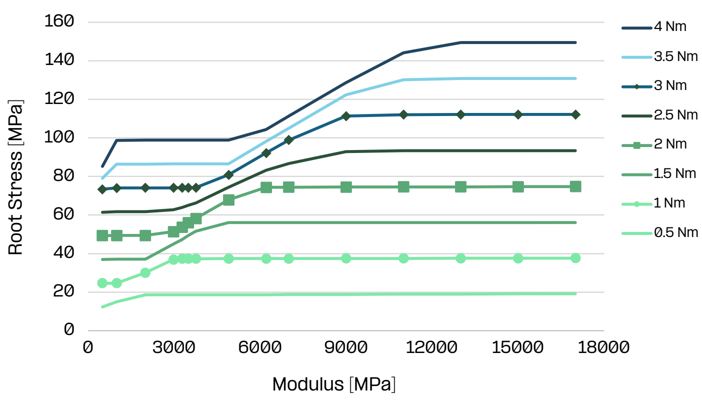

Figure 6b

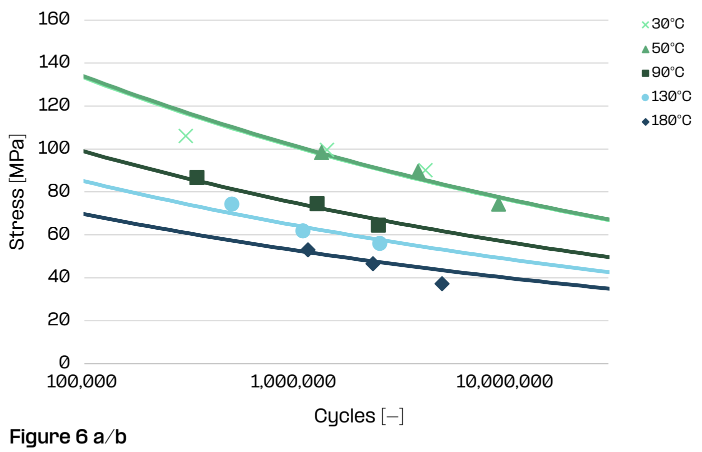

Figure 6 a/b
a) Root stress as a function of modulus for various torque levels calculated with KISSsoft and b) Converted torque to root stress results including S–N curves fits at various temperatures.

Now that the S–N curves on the gear specimens are generated, it is possible to fit Equation 2 on the experimental data. The data points hint towards a minor dependence of the slope m on temperature, but keep in mind only a few stress levels are available per temperature. However, as the solid lines in Figure 6b indicate an average value for m and only a temperature dependent pre–factor c_f also gives an accurate description. Note that the resulting pre–factors for the 30°C and 50°C datasets are identical.

Next, the evolution of the pre–factor c_f can be fitted using Equation 3, as illustrated in Figure 6a. It shows that also here the individual points can be described accurately by the model by only adjusting c_f. Only the value for the lowest temperature is underestimated. Note that the absolute value for c_f also depends on the value for m, and some inaccuracy was involved with that assumption already. For example, the data at 180°C suggests a steeper slope, and as a result the pre–factor from the model will not be able to describe every datapoint.

The data points hint towards a minor dependence of the slope m on temperature, but keep in mind only a few stress levels are available per temperature.

With Equation 2 and 3 parameterized (see Table 1) it is possible to describe the experimental data, as shown by the solid lines in Figure 7b, which indeed shows high accuracy (most data within a factor 3). Only for the highest temperature and long testing times, the model prediction is off, caused by wear at the gear teeth faces as confirmed by sample analysis after the test. The model now allows for gear lifetime predictions at any arbitrary temperature.

In this case, the contact temperature showed only little dependence on applied torque level and each T–N curve could be assumed isothermal. In the case a dataset displays a larger variation of contact temperature, one could combine different durability experiments at various environmental temperatures, torque levels and/or rotational speeds to obtain isothermal T–N curves.

m	8.3	–
ΔU	6535	J/mol
$c_{f,ref}$	511	MPa
T_{ref}	347.7	K

Table 1
Model parameters for predicting isothermal S–N curves.

Figure 7a

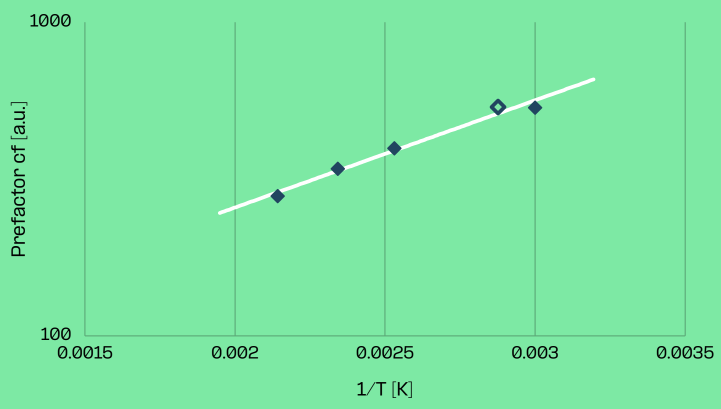

Figure 7b

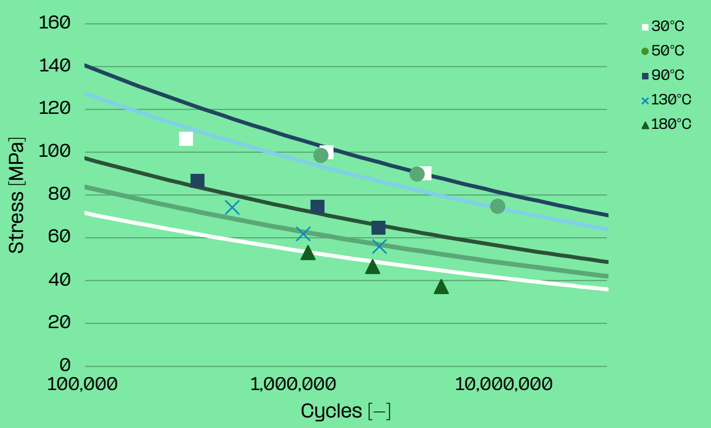

Figure 7 a/b
a) Fitting of the pre-factor cf as a function of temperature and b) prediction of the S–N curves with a temperature dependent pre-factor.

An approach has been developed, which allows the prediction of root fatigue failure, based on non-isothermal durability measurements on a gear tester. Isothermal root stress fatigue curves can be predicted by using a temperature dependent pre-factor. It is shown that the predictions are within a factor of 3 on lifetime, except for high temperatures and long testing times where wear starts playing a role. Envalior implemented this workflow for all the Stanyl grades suitable for gears and included all the necessary temperature dependent fatigue data in material cards for KISSsoft. Future work will focus on extending these material cards including closing the gap for wear related durability.

AUTHOR
Benjamin Van Weiss
CAE Expert/Scientist

This white paper is from VDI Conference Proceedings.

To learn more, contact us via Envalior.com.